PROCEEDINGS OF SPIE

SPIEDigitalLibrary.org/conference-proceedings-of-spie

How source/collector placement and subsurface absorbing layer affect time-resolved and phase/modulation-resolved photon migration

Steven L. Jacques, Andreas H. Hielscher, Lihong V. Wang, Frank K. Tittel

Steven L. Jacques, Andreas H. Hielscher, Lihong V. Wang, Frank K. Tittel, "How source/collector placement and subsurface absorbing layer affect time-resolved and phase/modulation-resolved photon migration," Proc. SPIE 1888, Photon Migration and Imaging in Random Media and Tissues, (14 September 1993); doi: 10.1117/12.154649

SPIE.

Event: OE/LASE'93: Optics, Electro-Optics, and Laser Applications in Scienceand Engineering, 1993, Los Angeles, CA, United States

How source/collector placement and subsurface absorbing layer affect time-resolved and phase/modulation-resolved photon migration.

Steven L. Jacques[1,2]
Andreas H. Hielscher[2]
Lihong Wang[1]
Frank Tittel[2]

[1]Laser Biology Research Laboratory
University of Texas M. D. Anderson Cancer Center
1515 Holcombe Blvd., Houston, TX 77030

[2]Department of Electrical and Computer Engineering
Rice University, Houston, TX 77030

1. ABSTRACT

The time-resolved reflectance of photons from a homogeneous tissue was modeled using a Monte Carlo simulation. The data was then converted by fast Fourier transform (FFT) into the frequency domain. In the frequency domain, the phase, Φ, and modulation, M, of collected light from a frequency-modulated light source was determined. A comparison of Monte Carlo and ciffusion theory was made for various separation distances between the source and collector on the tissue surface. The results showed that Monte Carlo and diffusion theory agreed in the time domain only for times larger than 500 ps after injection of an impulse of photons. In the frequency domain, Monte Carlo and diffusion theory agreed only if the probe separation, r, was at least 2 cm apart for $\mu_s' = \mu_s(1\text{-}g) = 5\ cm^{-1}$, or in dimensionless units $r\mu_s' > 10$.

The effect of buried absorbed is also tested in the time and frequency domains. A semi-infinite volume of absorber is placed at 0, 3 mm, 6 mm, or ∞ from the surface of a nonabsorbing tissue. The presence of a deep absorber on the time and frequency domain data show that attenuation of longer pathlength photons causes the phase of collected photons to reduce and the modulation of collected photons to increase. Both effects are indicative of the net shorter pathlength of the ensemble of collected photons.

2. INTRODUCTION

Photon migration in tissues can be described in either the time or frequency domains. We consider here the case of light escaping at the surface of a semi-infinite tissue. The time domain indicates the timecourse of collected light, called reflectance, by a collector at the surface in response to an impulse of injected light. The frequency domain indicates the phase and modulation of collected light from a a frequency-modulated source.

Several groups have introduced diffusion theory descriptions for photon migration in both the time and frequency domains [1,2,3,4]. Jacques [5] reported that time-resolved Monte Carlo simulations of photon migration did not agree with diffusion theory until after a time delay had elapsed. Sufficient time must pass to allow some scattering before photons behave according to diffusion theory. Therefore, in this study we sought to understand how this restriction in the time domain might translate into the frequency domain.

 0-8194-1115-9/93/$6.00

Furthermore, a second issue addressed in this paper is how an absorbing layer deep in the tissue will affect photon migration in both the time and frequency domains.

3. METHODS

3.1 Monte Carlo

A well-tested Monte Carlo simulation [6] was adapted to provide time-resolved photon propagation. Propagation was three-dimensional but photon escape as reflectance was collected in a cylindrically symmetric array. Photons escaping at radial position, r, within an incremental Δr of 1-mm were collected in an array R(r, t) with spatial resolution of 0.1 mm between 0-4 cm (40 intervals) and temporal resolution, Δt, of 25 ps over the range of 0-3.2 ns (or 128 time intervals). The results were expressed as the time-resolved local reflectance in $mm^{-1}ns^{-1}$.

3.2 Fast Fourier Transform (FFT)

To convert the data to the frequency domain, a fast fourier transform (FFT) [7] was used to convert a list of time-domain data, (t, h(t)), into a list of freqency-domain data, (Re($H(f_n)$), Im($H(f_n)$)), which were the real and imaginary components of the discrete Fourier transform, $H(f_n)$. The phase shift, ϕ, and the demodulation, M, for a photon density wave were then calculated:

$$\phi = \arctan\left(\frac{\mathrm{Im}\,(H(f_n))}{\mathrm{Re}\,(H(f_n))}\right) = \arctan\left(\frac{\mathrm{Im}\,(H_n)}{\mathrm{Re}\,(H_n)}\right) \tag{1}$$

$$M = \sqrt{\frac{\mathrm{Re}^2\,(H(f_n)) + \mathrm{Im}^2\,(H(f_n))}{\mathrm{Re}^2\,(H(0))}} = \sqrt{\frac{\mathrm{Re}^2(H_n) + \mathrm{Im}^2\,(H_n)}{\mathrm{Re}^2\,(H_0)}} \tag{2}$$

The 25-ps resolution, Δt, in the time domain determines the maximum frequency, $f_{max} = 1/(2\Delta t) = 20$ GHz, available in the frequency domain. For n data points in the time domain, the FFT yields n data points in the frequency domain. The resolution in the frequency domain is given by $\Delta f = f_{max}/n$. In order to increase the frequency resolution the common technique of "zero adding" was applied [8]. The time domain array with 128 points (3.2 ns) was expanded up to 1024 points (26.5 ns) by adding zeros into the R(r, t) array beyond 3.2 ns. The procedure is justified in this case by the fact that after 3.2 ns the time signal has decayed by several orders of magnitude. The frequency resolution achieved was $\Delta f = 39.1$ MHz.

When tissue absorption exerted sufficiently high attenuation on photon density wave propagation at high frequencies of modulation, the frequency-domain data fluctuated abnormally. Therefore, in the graphs of this report, we have truncated the upper range of the frequency-domain results when the behavior abnormally fluctuated.

3.3 Diffusion theory

The time-resolved diffusion theory of Patterson et al. [1], with a scaling factor k, was used to predict the behavior of photon migration in the model:

$$R(r, t) = k\,(4\pi Dc)^{-3/2}\, z_o t^{-5/2} \exp\left[-\frac{r^2 + z_o^2}{4Dct}\right] \exp(-\mu_a ct) \tag{3}$$

where D equals $[3(\mu_a + \mu_s(1-g))]^{-1}$, $z_o = [\mu_s(1-g)]^{-1}$, c is the speed of light in the tissue, μ_a is the absorption coefficient, μ_s is the scattering coefficient, and g is the anisotropy. k is a scaling factor required because diffusion theory does not exactly agree with the Monte Carlo simulations. The discrepancy occurs in the early reflected light near the injection point of the light source where diffusion theory is inaccurate. In other words, the total diffuse reflectance, $R_d = \iint R(r,t)2\pi r dr dt$, predicted by diffusion theory is slightly wrong, but the shape of the R(r, t) for later t is correct. Therefore k was introduced to cause diffusion theory to match Monte Carlo results at longer times greater than 0.5 ns. The scaled diffusion theory curve was then compared with Monte Carlo data. The scaled diffusion theory curve was also transformed into the frequency domain by the FFT for comparison with the transformed Monte Carlo data.

4. RESULTS

4.1 Comparing Monte Carlo and diffusion theory

Figure 1A depicts the model used for the comparision of Monte Carlo simulations and diffusion theory. The photon escape at 0.2, 1, 2, and 3 cm was analyzed. The tissue is a semi-infinite homegeneous medium with $\mu_a = 0.1$ cm^{-1}, $\mu_s = 62.5$ cm^{-1}, $g = 0.92$, and $\mu_s(1-g) = 5$ cm^{-1}.

Figure 1B shows the time-resolved behavior. The symbols denote Monte Carlo data and the solid lines denote the scaled diffusion theory. Fig. 1C shows a closeup of the data in the first ns. Note that the Monte Carlo data does not agree with diffusion theory at early times. The disagreement is especially large for the 0.2-cm escape site until about 50 ps. The curves for all escape sites persist in disagreeing with diffusion theory until roughly about 0.5 ns.

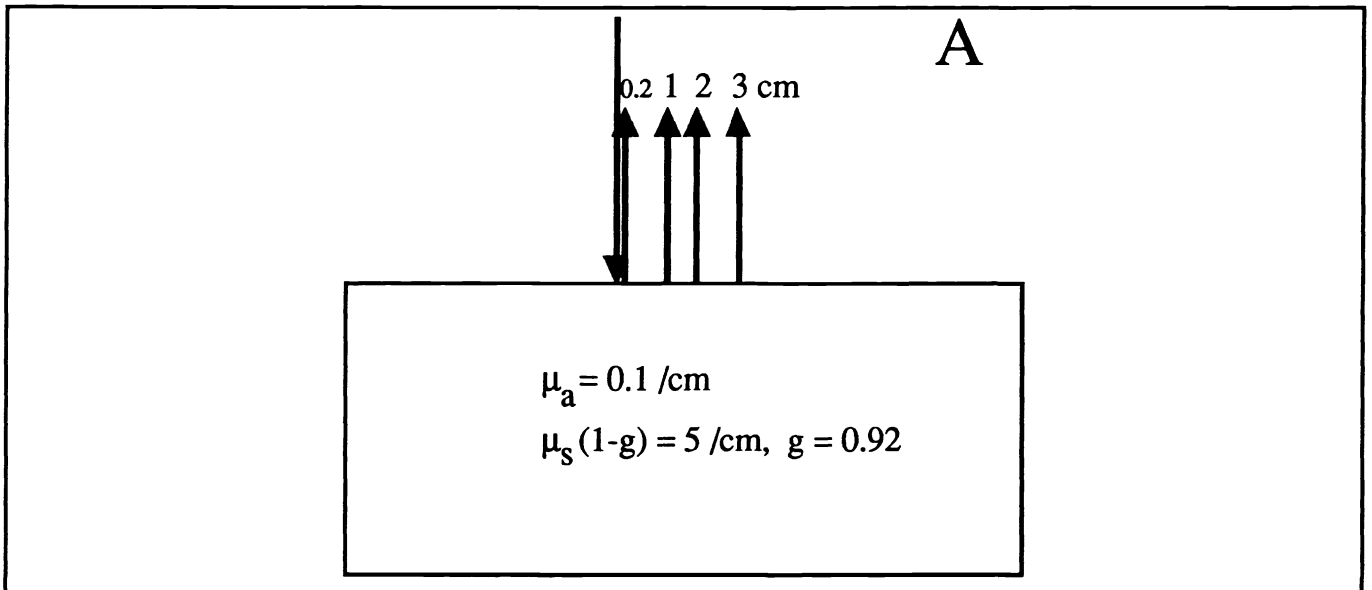

Fig. 1A: Model for simulation using both Monte Carlo and diffusion theory. The tissue is a semi-infinite homogeneous tissue with $\mu_a = 0.1$ cm^{-1}, $\mu_s(1-g) = 5$ cm^{-1}, $g = 0.92$. Light is incident at the origin and reflected light is collected at radial positions of 0.2, 1, 2, and 3 cm. The collection width, dr, is 1-mm.

Figure 1D shows the frequency-domain data in terms of the phase of collected photon density waves as a function of the modulation frequency. As the distance between source and collector

increases, the agreement between Monte Carlo and diffusion theory improves. At 3 cm, the agreement is quite good. Closer than 2 cm the disagreement is significant.

Figure 1E plots the modulation of escaping photon density waves as a function of modulation frequency. Again, Monte Carlo and diffusion theory agree when the distance between source and collector increases. Beyond 2 cm the agreement is good, but closer than 2 cm the disagreement is significant.

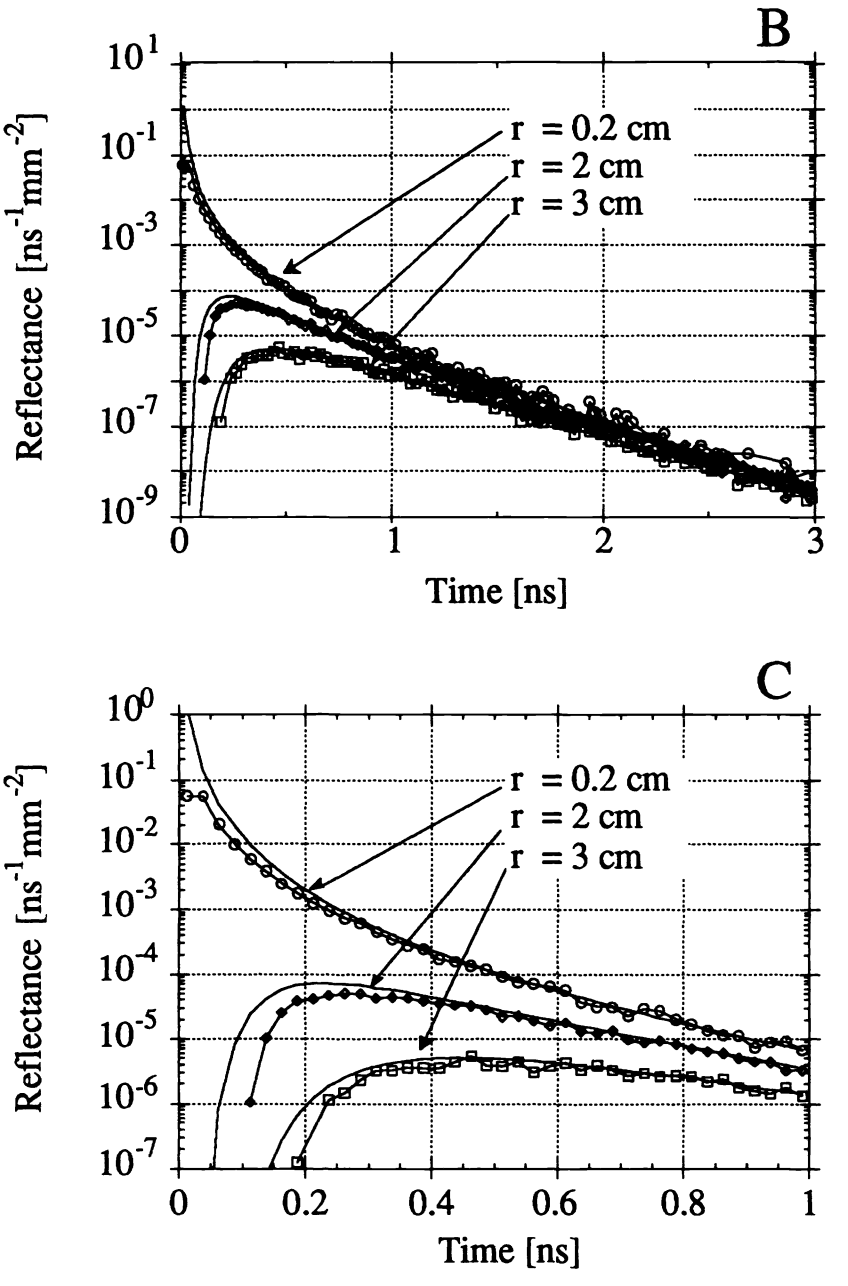

Fig. 1B: Time-resolved reflectance, for the model in Fig. 1A. Symbols indicate results of Monte Carlo simulation. Solid lines are diffusion theory. Fig. 1C is a closeup showing that Monte Carlo data does not agree with diffusion theory until about 0.5 ns.

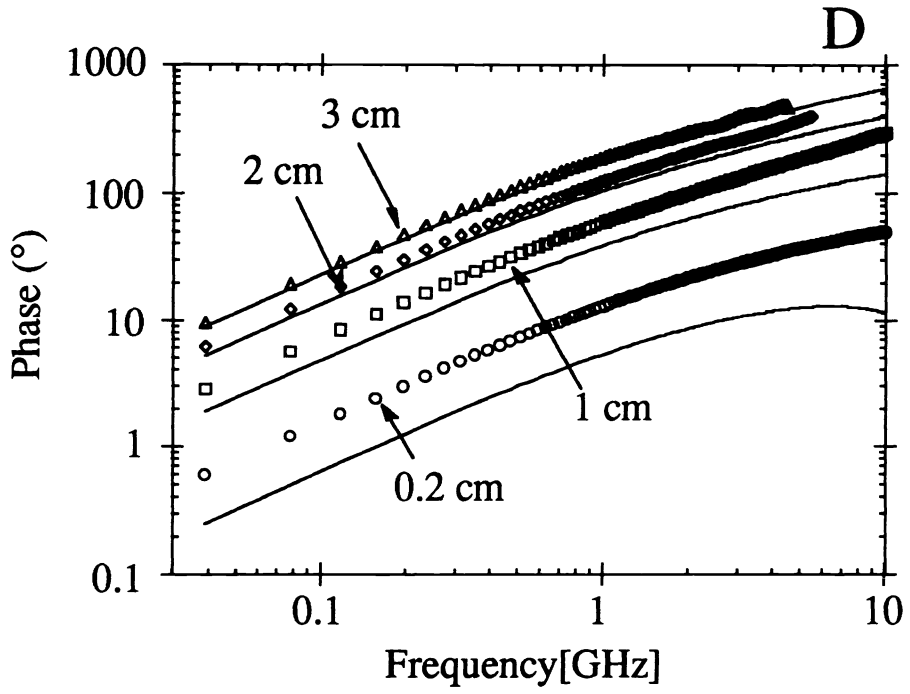

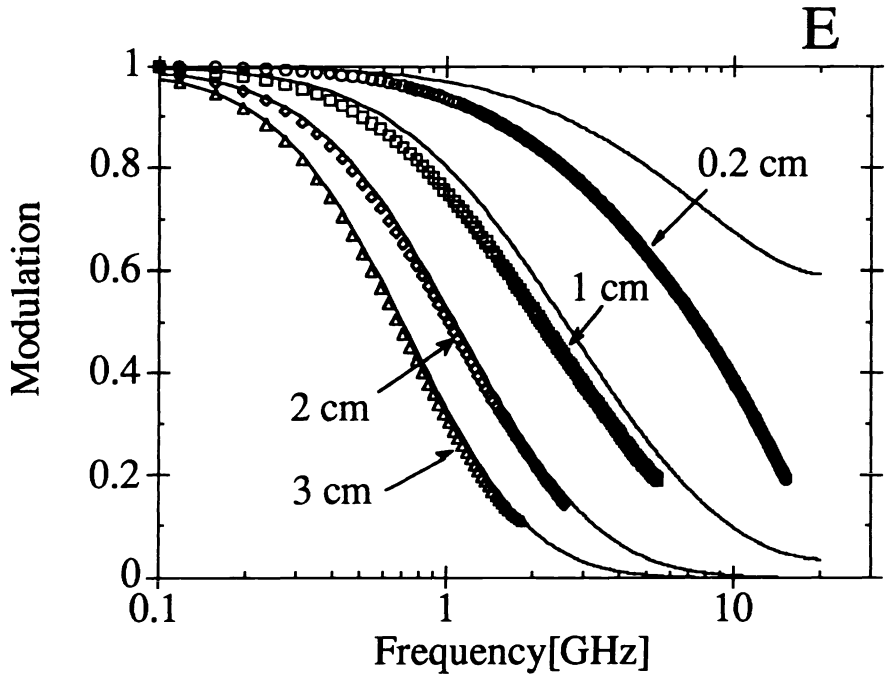

Fig. 1D, Phase Φ, and Fig. 1E, Modulation M, for model of Fig. 1A. Symbols are Monte Carlo simulation and solid curves are diffusion theory. There is significant disagreement between Monte Carl and diffusion theory for source/collector spacings of 0.2 and 1 cm, but good agreement for the 2 and 3 cm spacings.

4.2 Effect of buried absorber

Figure 2A shows the model used to examine the influence of a buried absorber. The tissue model is a planar multilayered medium. The upper tissue layer has not absorption. A deep absorbing layer has an absorption of 0.1 cm^{-1}. Both layers have scattering that is the same as Fig. 1, $\mu_s(1\text{-}g)$ equal 5 cm^{-1}. In **a**, the absorbing layer is infinitely far from the surface. In **b**, the absorbing layer is 6 mm from the surface. In **c**, the absorbing layer is 3 mm from the surface. In **d**, the entire tissue consists of the absorbing layer. These denotations, **a**, **b**, **c**, and **d**, are used in Figs. 2B-G.

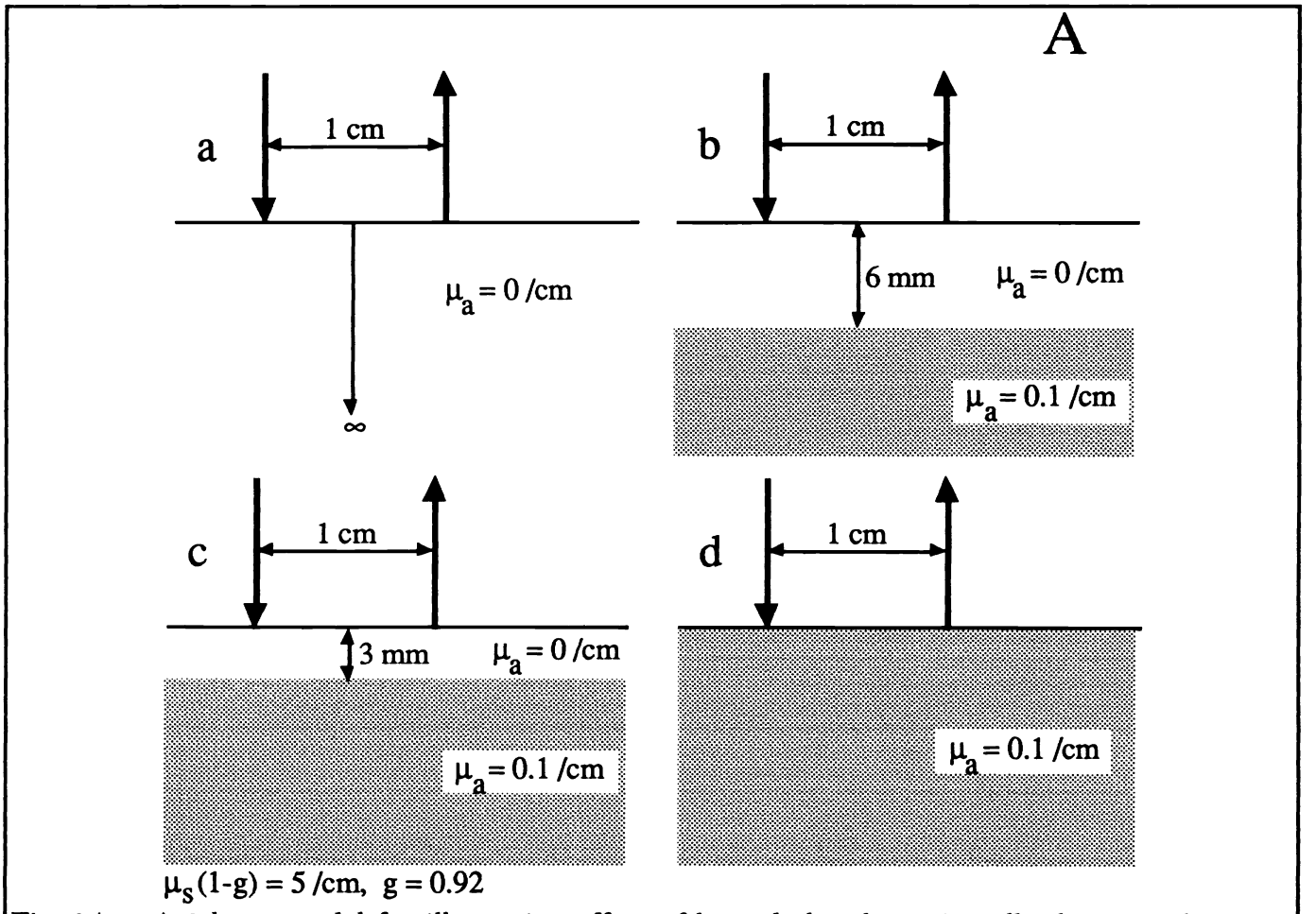

Fig. 2A: A 2-layer model for illustrating affect of buried absorber. Initially the tissue has zero absorption. The source and collector are separated by 1 cm. Then a semi-infinite volume of absorber (μ_a = 0.1 cm^{-1}) is brought closer to the surface. In **a**, there is no absorber. In **b**, the volume of absorber is 6 mm from the surface. In **c**, the absorber is 3 mm from the surface. In **d**, the entire tissue consists of absorber. These denotations, **a**, **b**, **c**, and **d**, are used in Figs. 2B-G.

Figure 2B shows the time-resolved reflectance. As the absorbing layer comes closer to the surface, the R(r, t) drops more quickly. Figure 2C shows a closeup of the first ns of data. Note that curve **b** does not deviate from curve **a** until about 0.22 ns. Apparently that is the time required before the presence of the absorbing layer exerts its influence from a 6-mm distance. As the absorbing laser moves closer to the surface, its effect is felt much sooner, within the first 100 ps.

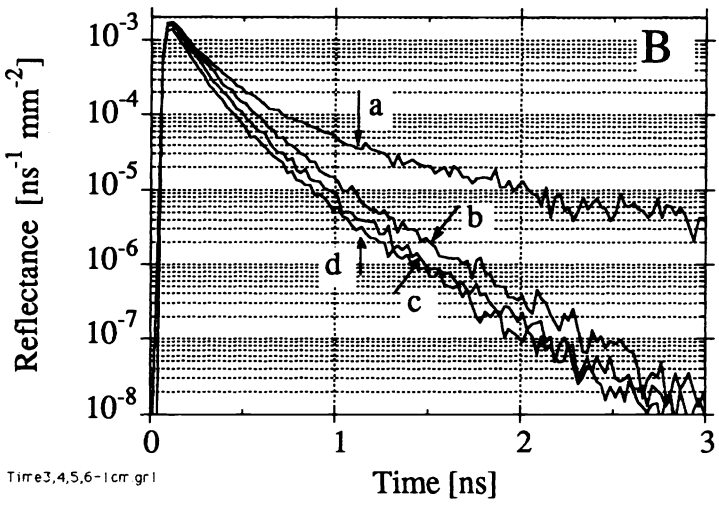

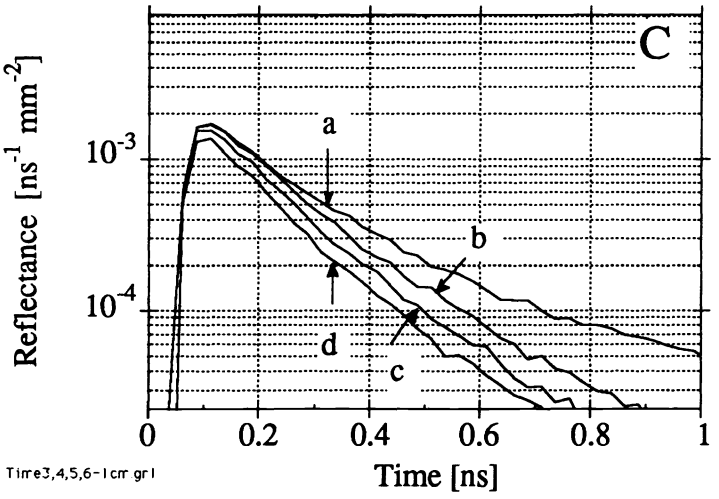

Fig. 2B: Time-resolved reflectance, for the model of Fig. 2A. Fig. 2C is a closeup showing that for case **b**, where the absorber is 6 mm from the surface, the data agrees with the no-absorber curve, **a**, until about 0.3 ns. Thereafter, **b** deviates from **a**. It takes 0.3 ns for the deep absorber to exert its influence on the time-resolved reflectance. Curves **c** and **d** deviate from curve **a** earlier.

Figure 2D shows the frequency domain results, expressed as the phase versus modulatio frequency. As the absorbing layer moves closer to the surface, the phase decreases. The presence of the absorbing layer is attenuating longer pathlength photons, which have a greater phase shift relative to the source. Therefore, the ensemble of photons collected 1 cm from the source becomes less dominated by long-pathlength photons as the absorbing layer moves toward the surface. Consequently, the observed average phase shift decreases in the presence of the absorbing layer. Figure 2E shows the phase difference, ΔPhase or ΔΦ, calculated by subtracting curve **a** from the others: (**b** - **a**), (**c** - **a**), and (**d** - **a**). The ΔPhase is negative as the net phase of the ensemble of collected photons moves toward earlier times. Note that the magnitude of the difference is maximal at a particular frequency, then returns to zero phase shift at very high frequencies.

Figure 2F shows expresses the frequency domain results in terms of the modulation, M, versus frequency. As the absorbing layer moves toward the surface, M increases. Attenuation of higher longer pathlength photons causes the ensemble of collected photons to shift toward shorter pathlengths and less loss of modulation. Figure 2G shows the ΔM, calculated by the differences (**b** - **a**), (**c** - **a**), and (**d** - **a**). The ΔM is positive as the net modulation of the ensemble decreases due to shorter net photon pathlength.

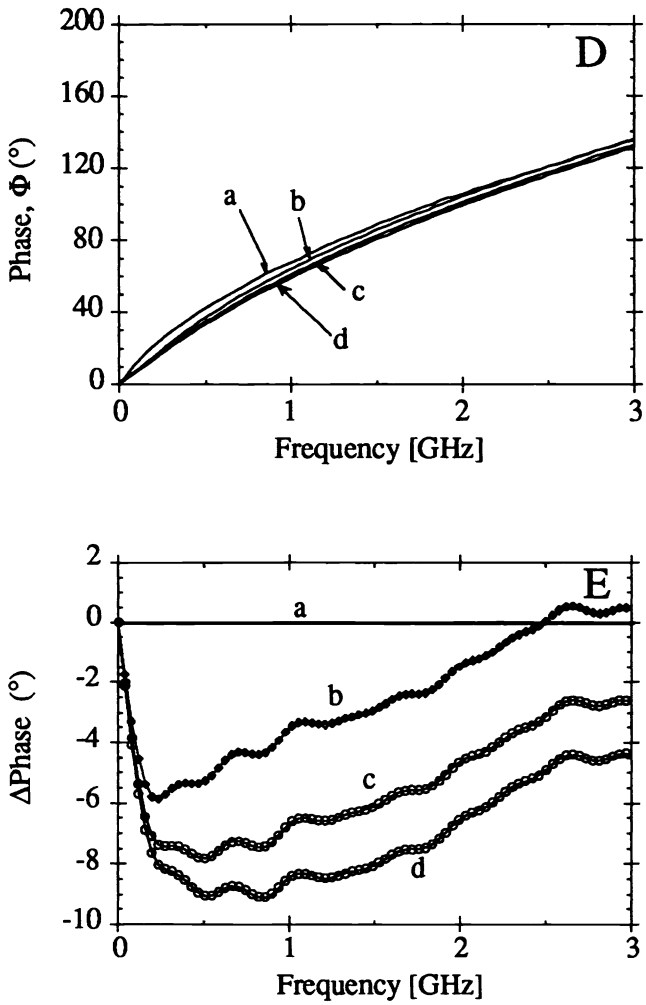

Fig. 2D: Frequency domain, based on Fourier transform of time-resolved Monte Carlo data for the model of Fig. 2A. The phase of a modulated light source is plotted as a function of modulation frequency. The presence of a deep absorbing volume attenuates longer pathlength photons and therefore the successfully collected photons reaching the collector have a shorter average pathlength and earlier average phase. In Fig. 2C, the phase difference, ΔPhase or ΔΦ, is calculated as (**b**-**a**), (**c**-**a**), and (**d**-**a**). The ΔPhase is negative because photons arrive with shorter average pathlengths and earlier average phase. Curves **a** and **d** denote homogeneous tissues with no absorber and 0.1 cm^{-1} absorption, respectively. Curves **b** and **c** are two layer models.

Note that ΔPhase is most significant at an intermediate frequency in the 0.2-1 GHz range, and lessens for both lower and higher frequencies.

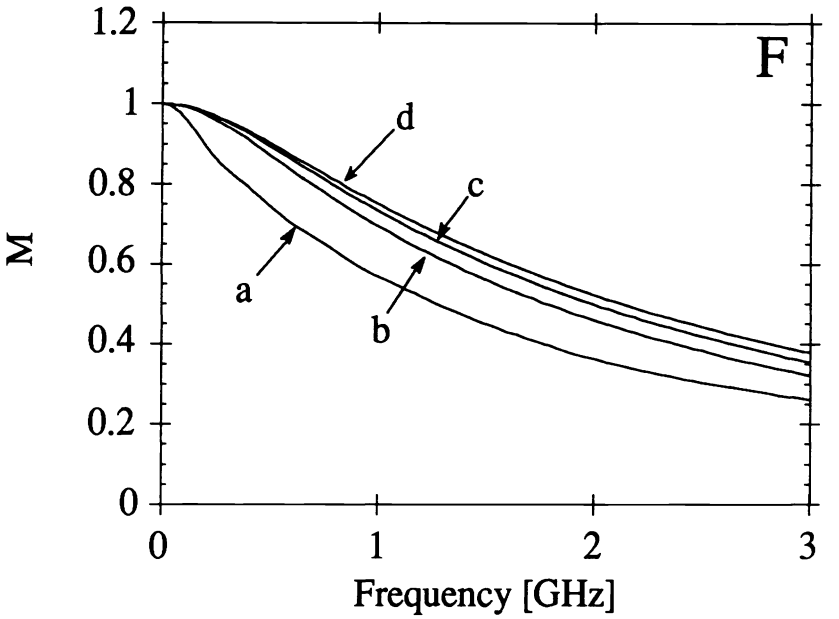

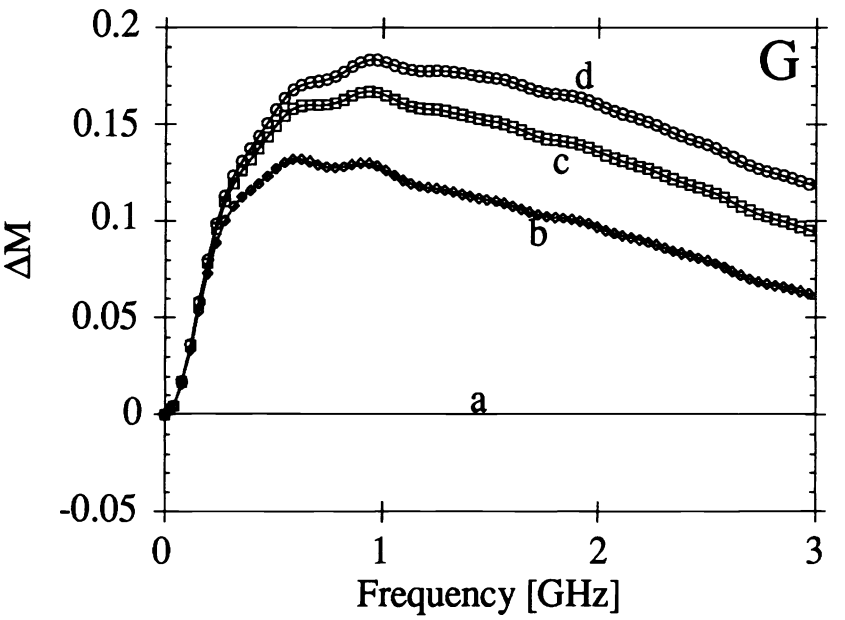

Fig. 2F: Frequency domain, based on Fourier transform of time-resolved Monte Carlo data for the model of Fig. 2A. Modulation, M, of the collected light from a frequency-modulated light source is shown as a function of modulation frequency. The presence of a deep absorber attenuates longer pathlength photons, and and therefore the successfully collected photons reaching the collector have a shorter average pathlength and less demodulation due to attenuation. Fig. 2G shows the change in modulation, ΔM, calculated (**b**-**a**), (**c**-**a**), and (**d**-**a**). The ΔM is positive. Curves **a** and **d** denote homogeneous tissues with no absorber and 0.1 cm^{-1} absorption, respectively. Curves **b** and **c** are two layer models.

5. DISCUSSION

5.1 Monte Carlo vs diffusion theory

The comparison of Monte Carlo and diffusion theory reminds us that it takes time (or equivalently, distance) for photons to become randomized so that diffusion theory becomes accurate. The use of the FFT to transform Monte Carlo results offers an approach toward the behavior of photon migration in the frequency domain. We had anticipated that in the frequency domain Monte Carlo and diffusion theory might agree at very low modulation frequencies and only disagree at high frequencies. However, our results show disagreement at all frequencies when the spacing between source and collector is too close. The results showed that Monte Carlo and diffusion theory agreed only if the probe separation, r, was at least 2 cm apart for μ_s' equal 5 cm^{-1}, or in dimensionless units $r\mu_s' > 10$.

5.2 Deep absorbing layer

The study of the absorbing layer illustrates that difference curves, ΔPhase or ΔM, can be useful in detecting the presence of an absorber. The behavior is understandable if one considers the signal as being due to an ensemble of photons with different pathlengths. As the absorbing layer moves toward the surface it affects the longer-pathlength photons in that ensemble. Shorter-pathlength photons begin to dominate the signal. Shorter-pathlength photons experience less phase shift and less loss of modulation. Therefore the phase of the detected signal decreases and the modulation increases.

6. ACKNOWLEDGEMENTS

This study was supported by the Department of Energy (DE-FG05-91ER617226), the Department of the Navy (N00015-91-J-1354), and the NIH (R29-HL45045).

7. REFERENCES

1 Patterson MS, B Chance, BC Wilson, "Time resolved refletance and transmittance for the non-invasive measurment of tissue optical properties," *Applied Optics* 28, 2331ff, 1989.

2 Patterson MS, JD Moulton, BC Wilson, KW Berndt, "Frequency domain reflectance for the determination of the scattering and absorption properties of tissues," *Applied Optics* 30, 4474ff, 1991.

3 Fishkin J, E Gratton, MJ vande Ven, WW Mantulin, "Diffusion of intensity modulated near-infrared light in turbid media," *SPIE* Vol. 1431, *Time-Resolved Spectroscopy and Imaging of Tissues*, p. 121ff, 1991.

4 Tromberg BJ, LO Svaasand, TT Tsay, RC Haskell, MW Berns, "Optical property measurements in turbid media using frequency domain photon migration," *SPIE* Vol. 1525, *Future Trends in Biomedical Applications of Lasers*, p. 52-58, 1991.

5 Jacques SL, "Time-resolved reflectance spectroscopy in turbid tissues," *IEEE Trans. on Biomed. Eng.* 36, p. 1155ff, 1989.

6 Wang L, SL Jacques, *Monte Carlo Modeling of Light Transport in Multi-Layered Tissues in Standard C*, Laser Biology Research Laboratory, University of Texas, 1515 Holcombe Blvd., Houston, TX 77030 (E-mail: slj@odin.mda.uth.tmc.edu).

7 WH Press, BP Flannery, SA Teukolsky, WT Vetterling: *Numerical recipes in C.* Cambridge University Press, 1988.

8 Brigham EO, *The Fast Fourier Transform*, Prentice-Hall, Inc., Englewood Cliffs, NJ, 1974.